A New Macrocyclic N_3S_2 Ligand and Its Nickel(II), Cobalt(II), Rhodium(III)-103, and Rhodium(III)-105 Complexes

Dawn C. Goodman,[†] Joseph H. Reibenspies,[†] Niranjan Goswami,[‡] Silvia Jurisson,*[,‡] and Marcetta Y. Darensbourg*[,†]

Contribution from the Department of Chemistry, Texas A&M University, College Station, Texas 77843-3255, and Department of Chemistry, University of Missouri, Columbia, Missouri 65211

Received December 4, 1996[⊗]

Abstract: The synthesis, structural characterization, and electrochemical properties of N_3S_2-ligated metal complexes of the ligand 4,10-dithia-1,7,13-triazabicyclo[11.3.3]nonadecane are described. Complexes of Ni^{II}, Co^{II}, and Rh^{III} have been characterized by X-ray crystallography as six-coordinate complexes of the pentadentate ligand with Cl^- anions occupying the position *trans* to the secondary amine donor. In addition, the chelation of the N_3S_2 donor ligand to the reactor-produced radionuclide ^{105}Rh was shown to give a single product in high yield (>98% at pH 5). The ligand is prepared by the template reaction of (*N*,*N*′-bis(2-mercaptoethyl)-1,5-diazacyclooctane)nickel(II), **Ni-1**, with bis(2-chloroethyl)amine, yielding (*S*,*S*′-(3-aza-1,5-pentanediyl)-*N*,*N*′-bis(2-mercaptoethyl)-1,5-diazacyclooctane-*N*,*N*′,*N*″,*S*,*S*′)nickel(II) chloride, [Ni(amine)Cl]Cl. Removal of nickel from [Ni(amine)Cl]Cl and subsequent reaction of the ligand with $CoCl_2$ or $RhCl_3{\cdot}xH_2O$ afforded (*S*,*S*′-(3-aza-1,5-pentanediyl)-*N*,*N*′-bis(2-mercaptoethyl)-1,5-diazacyclooctane-*N*,*N*′,*N*″,*S*,*S*′)cobalt(II) chloride, [Co(amine)Cl]Cl, $C_{14}H_{29}N_3S_2CoCl_2{\cdot}1.75MeOH$, and (*S*,*S*′-(3-aza-1,5-pentanediyl)-*N*,*N*′-bis(2-mercaptoethyl)-1,5-diazacyclooctane-*N*,*N*′,*N*″,*S*,*S*′)rhodium(III) chloride, [Rh(amine)Cl]Cl_2, $C_{14}H_{29}N_3S_2RhCl_3$, respectively. The blue complex [Ni(amine)Cl]Cl, $C_{14}H_{29}N_3S_2NiCl_2{\cdot}MeOH$, contains nickel in an octahedral environment of N_3S_2Cl donors and crystallizes in the monoclinic space group $P2_1/c$ with $a = 13.278(3)$ Å, $b = 11.976(4)$ Å, $c = 12.928(4)$ Å, $\beta = 102.17(2)°$, and $Z = 4$. The complex [Co(amine)Cl]Cl is fuchsia and crystallizes in the monoclinic space group $P2_1/n$ with $a = 10.321(2)$ Å, $b = 7.892(1)$ Å, $c = 27.684(3)$ Å, $\beta = 96.91(1)°$, and $Z = 4$. Yellow crystals of [Rh(amine)Cl]Cl_2, $C_{14}H_{29}N_3S_2RhCl_3$, were determined to be in the monoclinic space group $C1c1$ with $a = 9.655(2)$ Å, $b = 16.805(4)$ Å, $c = 11.756(3)$ Å, $\beta = 96.29(2)°$, and $Z = 4$.

Introduction

The well-known ability for *cis*-dithiolate complexes of nickel(II) diamine derivatives to template the synthesis of thioethers and thioether macrocycles[1] has been extensively exploited for the sterically constrained (*N*,*N*′-bis(2-mercaptoethyl)-1,5-diazacyclooctane)nickel(II), **Ni-1**, complex (eq 1).[2−4]

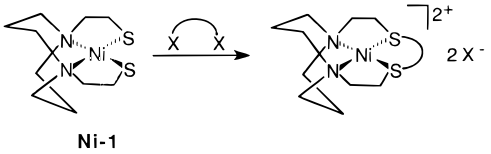

(1)

Ni-1

Particularly interesting was the possibility of generating five-coordinate Ni^{II} complexes from the reaction of **Ni-1** with dihaloalkanes, functionalized with heteroatom donors. In fact, a study of the product generated from reaction of **Ni-1** with $(BrCH_2CH_2)_2O$ revisited the 6 or 4 coordination number preference of nickel(II) as dictated by solvent, counter ion, and chair/boat vs chair/chair configurations of the diazacyclooctane, daco, backbone (eq 2).[3] As depicted in eq 2, there was no evidence for the five-coordinate N_2S_2O intermediate. Further

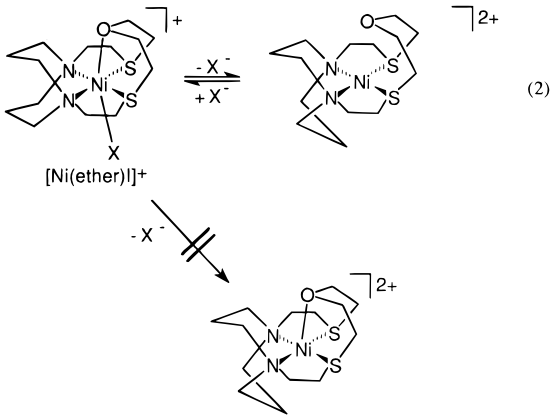

(2)

examination of factors that influence coordination at the nickel center prompted the synthesis of an N_3S_2 donor set from the reaction of **Ni-1** with $(ClCH_2CH_2)_2NH$ (eq 3). The N_3S_2 donor

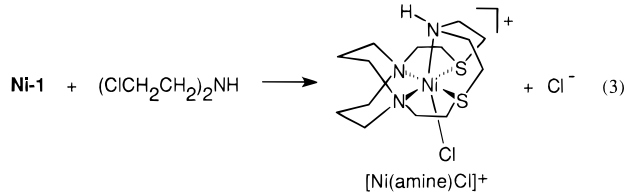

(3)

set was interesting for a comparison of coordination chemistry between O and N as axial donors for Ni^{II}, and also for a comparison of metallic derivatives, namely, Co^{II} and Rh^{III}.

As implicated by the stick drawings of metal-bound daco, the β-methylene group of the boat conformer of the metalla-

[†] Texas A&M University.
[‡] University of Missouri-Columbia.
[⊗] Abstract published in *Advance ACS Abstracts,* May 1, 1997.

(1) Thompson, M. C.; Busch, D. H. *J. Am. Chem. Soc.* **1964**, *86*, 3651.
(2) Darensbourg, M. Y.; Font, I.; Pala, M.; Reibenspies, J. H. *J. Coord. Chem.* **1994**, *32*, 39.
(3) Darensbourg, M. Y.; Font, I.; Mills, D. K.; Pala, M.; Reibenspies, J. H. *Inorg. Chem.* **1992**, *31*, 4965.
(4) Goodman, D. C., Buonomo, R. M.; Farmer, P. J.; Reibenspies, J. H.; Darensbourg, M. Y. *Inorg. Chem.* **1996**, *35*, 4029.

S0002-7863(96)04187-X CCC: $14.00

Scheme 1

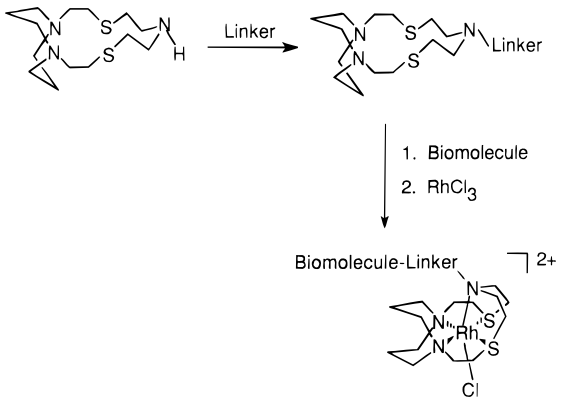

diazacyclohexane ring is positioned sufficiently close to the metal as to be in "agostic" interaction range.[5] Indeed, one of the first examples of C−H activation involved an N_2O_2 ligand based on daco, 1,5-diazacyclooctane-*N*,*N*′-diacetic acid (dacoda).[5d] With a strong field axial ligand, oxidation of the Co^{II} complex to Co^{III} resulted in a structure exhibiting a Co−(C−H) agostic interaction which, on addition of base, led to Co−C bond formation concomitant with heterolytic C−H bond cleavage. This interesting C−H bond activation has not been further explored and remains a long-term goal for the new $N_3S_2Co^{II}$ complex.

Numerous ligands containing combinations of N and S donors have been synthesized and chelated to metals with radioactive isotopes for potential use as imaging agents and radiotherapeutics.[6] The reactor-produced radionuclide ^{105}Rh has nuclear properties suitable for use in therapeutic radiopharmaceuticals (E_β(max) = 560 keV (70%), 250 keV (30%); E_γ = 306 keV (5%), 319 keV (19%); $t_{1/2}$ = 36 h).[7] The availability of high specific activity ^{105}Rh and the kinetic inertness of d^6 Rh^{III} complexes increase its potential utility. Thus, suitable ligand systems which will ultimately serve as bifunctional chelates to which a targeting biomolecule is appended (*e.g.*, peptide, monoclonal antibody fragment, etc.) are synthetic goals (Scheme 1). The 36 h half-life of ^{105}Rh makes it preferable to append the targeting biomolecule to the ligand prior to complexation with ^{105}Rh. With this condition included, the ^{105}Rh complexation reaction with the ligand must proceed in high yield under relatively mild conditions (>90% yield, *ca.* <2 h), with the temperature limit dependent on the particular biomolecule.

The development of potential ^{105}Rh radiopharmaceuticals has primarily focused on Rh^{III} complexes with nitrogen and oxygen donor ligands, such as amine−phenols,[8] amines,[9] and porphyrins.[10] However, the formation of the ^{105}Rh complexes with these ligands required harsh conditions (aqueous reflux) and long reaction times, and high yields were not always obtained.[8−10] Recently, a macrocyclic tetrathioether ^{105}Rh complex was reported that showed good stability under biological conditions,[11a] consonant with the fact that cyclic thioethers as well as polyaza macrocyclics are known to efficiently complex rhodium.[11b,c] Since only a few N/S donor complexes of Rh^{III} are reported,[11d,e] it seemed appropriate to explore the mixed donor N_3S_2 macrocycle, as illustrated in eq 3, which offers both the excellent donors expressed in daco and thioethers and a secondary amine as a site for functionalization which would allow conjugation to a biomolecule. Herein we report the nickel-templated synthesis of 4,10-dithia-1,7,13-triazabicyclo[11.3.3]nonadecane as well as the protocol developed for its release and use as a chelating agent for other metals, including ^{105}Rh.

Experimental Section

General Procedures. Standard Schlenk or syringe techniques using nitrogen (passed through a drying tube of $CaSO_4$, molecular sieves, and NaOH) and an argon glovebox (Vacuum Atmospheres) were employed. Solvents were dried according to published procedures and distilled under N_2.[12] Acetonitrile was distilled once from CaH_2 and twice from P_2O_5 and was freshly distilled from CaH_2 immediately before use. The following starting materials were of reagent grade and used as received: bis(2-chloroethyl)amine hydrochloride (Aldrich), $NaBH_4$ (Aldrich), NaOH (Mallinckrodt), KCN (Fisher), K_2CO_3 (EM).

^{105}Rh was prepared at the Missouri University Research Reactor (MURR) by bombardment of ^{104}Ru metal (Isotec, Inc.) for 3 days at a thermal neutron (n) flux of 8×10^{13} n/(cm^2 s). The irradiated Ru target was oxidized with Cl_2 and separated from ^{105}Rh by the method previously described.[13] Approximately 5−10 mCi (185−370 MBq) of $^{105}Rh^{III}$ as the chloride in 2 mL of HCl acidified solution (pH *ca.* 1) was supplied for these studies. This rhodium(III)-105 chloride reagent is considered to be a mixture of anionic chloro−aqua species, as determined by electrophoresis, presumably the tetra-, penta- and hexachlororhodium(III)-105 anions.[11] Standard radiation safety procedures were followed at all times when ^{105}Rh was handled.

Physical Measurements. UV−vis spectra were measured with a Hewlett-Packard 8452A diode array spectrophotometer and quartz cells of light path length 1.00 cm. Cyclic voltammograms were recorded on a BAS-100A electrochemical analyzer using $Ag^0/AgNO_3$ reference and glassy carbon working electrodes with 0.1 M tetra-*n*-butylammonium hexafluorophosphate in CH_3CN, DMF, or CH_2Cl_2. Alternatively, a Ag^0/AgCl reference and glassy carbon working electrodes with 0.1 M LiBr in EtOH were used. EPR data on frozen solutions were obtained at 10 K on a Bruker ESP 300 spectrometer equipped with an Oxford Instruments ER910A cryostat. Elemental analyses were carried out by Galbraith Laboratories, Knoxville, TN. X-ray crystallographic data were obtained on a Rigaku AFC5-R single-crystal X-ray diffractometer. Mass spectral analyses were performed at the Labora-

(5) (a) Legg, J. I.; Neilson, D. O.; Smith, D. L.; Larsen, M. L. *J. Am. Chem. Soc*. **1968**, *90*, 5030. (b) Neilson, D. O.; Larsen, M. L.; Willett, R. D.; Legg, J. I. *J. Am. Chem. Soc.* **1971**, *93*, 5079. (c) Averill, D. F.; Legg, J. I.; Smith, D. L. *Inorg. Chem.* **1972**, *11*, 2344. (d) Broderick, W. E.; Kanamori, K.; Willett, R. D.; Legg, J. I. *Inorg. Chem.* **1991**, *30*, 3875.

(6) (a) Meegalla, S.; Plössl, K.; Kung, M.-P.; Stevenson, D. A.; Liable-Sands, L. M.; Rheingold, A. L.; Kung, H. F. *J. Am. Chem. Soc*. **1995**, *117*, 11037. (b) Marzilli, L. G.; Banaszczyk, M. G.; Hansen, L.; Kuklenyik, Z.; Cini, R.; Taylor, A. T. *Inorg. Chem.* **1994**, *33*, 4850. (c) Schultze, L. M.; Todaro, L. J.; Baldwin, R. M.; Byrne, E. F.; McBride, B. J. *Inorg. Chem.* **1994**, *24*, 5579. (d) Spies, H.; Glaser, M.; Pietzsch, H.-J.; Hahn, F. E.; Kintzel, O.; Lügger, T. *Angew. Chem., Int. Ed. Engl.* **1994**, *33*, 1354. (e) Marchi, A.; Marvelli, L.; Rossi, R.; Magon, L.; Bertolasi, V.; Ferretti, V.; Gilli, P. *J. Chem. Soc., Dalton Trans.* **1992**, 1485. (f) White, D. J.; Küppers, H.-J.; Edwards, A. J.; Watkin, D. J.; Cooper, S. R. *Inorg. Chem.* **1992**, *31*, 5351. (g) Edwards, D. S.; Liu, S.; Poirier, M. J.; Zhang, Z.; Webb, G. A.; Orvig, C. *Inorg. Chem.* **1994**, *33*, 5607. (h) Chi, D. Y.; Wilson, S. R.; Katzenellenbogen, J. A. *Inorg. Chem.* **1995**, *34*, 1624.

(7) (a) Troutner, D. E. *Nucl. Med. Biol*. **1987**, *14*, 171. (b) Volkert, W. A.; Goeckler, W. F.; Ehrhardt, G. J.; Ketring, A. R. *J. Nucl. Med*. **1991**, *32*, 174.

(8) Pillai, M. R. A.; John, S. S.; Troutner, D. E. *Bioconjugate Chem*. **1990**, *2*, 191.

(9) (a) Pillai, M. R. A.; Lo, J. M.; John, C. S.; Troutner, D. E. *Nucl. Med. Biol*. **1990**, *17*, 419. (b) Kruper, W. J., Jr.; Pollock, D. K.; Fordyce, W. A.; Fazio, M. J.; Inbasekaran, M. N. U.S. Patent No. 4,994,560, Feb 19, 1991. (c) Collman, J. P.; Schneider, P. W. *Inorg. Chem.* **1966**, *8*, 1380.

(10) Pillai, M. R. A.; Lo, J. M.; Troutner, D. E. *Int. J. Radiat. Appl. Instrum., Part A, Appl. Radiat. Isot*. **1990**, *41*, 69.

(11) (a) Venkatesh, M.; Goswami, N.; Volkert, W. A.; Schlemper, E. O.; Ketring, A. R.; Barnes, C. L.; Jurisson, S. *Nucl. Med. Biol*. **1996**, *23*, 33. (b) Cooper, S. R. *Acc. Chem. Res.* **1988**, *21*, 141. (c) Blake, A. J.; Reid, G.; Schröder, M. *Polyhedron* **1990**, *24*, 2925. (d) Li, N.; Ochrymowycz, L. A.; Higginbotham, C.; Struttman, M.; Abrams, M. J.; Vollano, J. F.; Skerlj, R. T.; Ketring, A. R.; Volkert, W. A. J. *Labelled Compd. Radiopharm., Symp. Abstr*. **1995**, *37*, 426. (e) McCrindle, R.; Gerguson, G.; McAlees, A. J.; Parvez, M.; Ruhl, B. L.; Stephenson, D. K.; Wieckowski, T. *J. Chem. Soc., Dalton Trans.* **1986**, 2351.

(12) Gordon, A. J.; Ford, R. A. *The Chemist's Companion*; Wiley and Sons: New York, 1972; pp 429−436.

(13) Grazman, B.; Troutner, D. E. *Int. J. Radiat. Appl. Instrum., Part A, Appl. Radiat. Isot*. **1988**, *39*, 257.

tory for Biological Mass Spectroscopy at Texas A&M University. Positive ion fast atom bombardment mass spectra were recorded in thioglycerol and 4-nitrobenzyl alcohol (NBA) matrices using a VG-70S spectrometer with a xenon source having a particle energy of 10 keV. Data were collected by a VG11-250J data system. NMR spectra were obtained on a Varian XL-400 FT-NMR spectrometer.

Radiochemical Analyses. Radiochemical analyses were accomplished using silica-coated TLC plates (Baker), paper electrophoresis (Gelman Sciences, Inc.), and MgO adsorption. Since the uncomplexed rhodium(III)-105 chloride reagent adsorbs to MgO while ^{105}Rh complexes generally do not adsorb, this method was used to rapidly assess the percent of uncomplexed ^{105}Rh remaining in the samples.[14] Quantitation of the distribution of radioactivity on TLC plates or on paper was measured using a radiochromatographic strip scanner (BioScan System 200) or by sectioning the paper in 1-cm increments and counting in a NaI(Tl) well counter. Silica TLC plates were developed with either 0.9% aqueous NaCl (normal saline) or chloroform−methanol (50/50). The R_f value of the uncomplexed control rhodium(III)-105 chloride reactant was 0.9−1.0 when saline was the eluent. The R_f for the ^{105}Rh−N_3S_2 complex was 0.3−0.6 (streaking observed to solvent front) which is consistent with that of the ^{103}Rh−N_3S_2 complex with saline as the eluent. When chloroform−methanol was used as the eluent, the R_f value for the uncomplexed control rhodium(III)-105 chloride was 0. Although the ^{103}Rh−N_3S_2 complex is sparingly soluble in chloroform−methanol, an R_f value was determined to be 0.93. Paper electrophoresis was performed at 10 V/cm for 1 h using Whatman no. 1 paper strips and pH 7.0 phosphate/citrate buffer (0.05 M Na_2HPO_4/0.02 M citrate) as the electrolyte. The results using MgO adsorption were found to be consistent with the results obtained by electrophoresis and TLC.

Potentiometric Measurements. All pH calibrations were performed with standardized dilute HCl. Both pH and p[H] values/terms are used; while the former is a measure of hydrogen ion activity, the latter allows direct measurement of hydrogen ion concentration by keeping the solution ionic strength constant (maintained at 0.10 M with KCl). Thus, p[H] is defined as $-\log [H^+]$.[15]

Potentiometric studies were carried out with a Corning Model 250 pH meter fitted with blue-glass and calomel reference electrodes. Aqueous solutions of ligand (0.0101 M 4,10-dithia-1,7,13-triazabicyclo-[11.3.3]nonadecane hydrochloride (5 mL)) and electrolyte (5 mL of 1.0 M KCl, doubly distilled H_2O (38 mL), and 0.02535 M HCl (2 mL)) were placed in a 50 mL jacketed cell thermostated at 25.0 ± 0.05 °C by a refrigerated circulating water bath. The cell was maintained under anaerobic conditions, established by a stream of prepurified nitrogen. Experimental runs were carried out by adding increments (0.1 mL) of standard base (0.1009 M KOH) to the solution of the acid (hydrochloride) form of the macrocycle and the above-mentioned components. The p[H] profile was determined by utilizing at least 10 points per protonation equivalent. The range of accurate p[H] measurement was determined to be 2−12. In the potentiometric determination, the σ_{fit},[15] which measures the deviation of the experimental curve and the curve calculated from the equilibrium constants, was less than 0.01 pH unit. A variation on log K of 0.01−0.02 was required to produce an observable deviation in the distribution curves.

Calculations. Equilibrium constants were calculated with the program BEST.[15] XYPREP and LSQFIT were used for computation of titration curves.[15] Species distribution curves were computed and plotted using and SPE and SPEPLOT.[15] The log K_w for the system, defined in terms of $\log[-([H^+][OH^-])]$, was found to be −13.8 at the ionic strength employed and was constant during refinements. Details of the potentiometric method have been described.[15]

Syntheses. The **Ni-1** complex was synthesized according to the published procedure[16] and used as isolated following purification by silica (60−200 mesh) column chromatography (12 × 1 in. column, MeOH as eluent) and removal of methanol via vacuum.

(*S*,*S*′-(3-Aza-1,5-pentanediyl)-*N*,*N*′-bis(2-mercaptoethyl)-1,5-diazacyclooctane-*N*,*N*′,*N*″,*S*,*S*′)nickel(II) Chloride, [Ni(amine)Cl]Cl. A saturated aqueous solution of potassium carbonate was added to bis-(2-chloroethyl)amine hydrochloride until pH ∼10. Bis(2-chloroethyl)-amine was extracted into diethyl ether. The ether extracts were dried over Na_2SO_4 for a minimum of 30 min and filtered through Celite; solvent was removed via vacuum. The resulting clear to yellow oil (0.29 mL, 2.04 mmol) was transferred by syringe to a purple acetonitrile solution (50 mL) of **Ni-1** (0.119 g, 0.41 mmol). The solution was stirred under N_2 for 14 h at 60−65 °C, over which period color changes from purple to brown, and finally to green, were observed. Finally, a hygroscopic blue precipitate which stuck to the walls of the flask formed. The supernatant was removed by a cannula; the remaining solid was washed with diethyl ether (3 × 10 mL). This product was dissolved in anhydrous MeOH (∼10 mL), and blue crystals of [Ni-(amine)Cl]Cl·MeOH suitable for X-ray analysis were formed from diethyl ether diffusion (yield 46%). Anal. Calcd (Found) for $C_{14}H_{29}N_3S_2NiCl_2$•MeOH•H_2O: C, 37.3 (37.07); H, 7.30 (6.96). Inclusion of a water molecule is warranted by the compound's hygroscopic nature. FTIR (KBr pellet): ν [cm^{-1}] = 3470, 3099, 1080. UV−vis [λ_{max}, nm (ϵ)]: in MeOH, 366 (85), 568 (38); in CH_2Cl_2, 384 (40), 596 (25).

4,10-Dithia-1,7,13-triazabicyclo[11.3.3]nonadecane. The metal-free amine ligand was obtained by dissolving the [Ni(amine)Cl]Cl complex in a minimal amount of distilled H_2O and adding solid KCN until the solution was decolorized or yellow (at least 5 equiv). The ligand was extracted into diethyl ether and obtained as a colorless to yellow oil upon solvent removal by vacuum. ^{1}H NMR ($CDCl_3$): δ 2.84 (m, 12H), 2.72 (t, 4H), 2.64 (m, 8H), 1.8 (br m, 2H), 1.48 (br m, 2H). FAB$^+$ mass spectroscopy: *m*/*z* 304, 167, 141, 127, 112. A white, solid, hygroscopic form of the ligand may be obtained by dissolving the ligand in CH_2Cl_2 and bubbling HCl(g) through the solution for 15 min. Excess HCl was removed by bubbling N_2(g) through the solution.

(*S*,*S*′-(3-Aza-1,5-pentanediyl)-*N*,*N*′-bis(2-mercaptoethyl)-1,5-diazacyclooctane-*N*,*N*′,*N*″,*S*,*S*′)cobalt(II) Chloride, [Co(amine)Cl]Cl. 4,10-Dithia-1,7,13-triazabicyclo[11.3.3]nonadecane (0.087 g, 0.29 mmol), isolated as described above, was dissolved in dry MeOH (5 mL); to this a pink solution of $CoCl_2$ (0.034 g, 0.26 mmol) in dry MeOH (5 mL) was added via cannula. The reaction solution was stirred at 22 °C for 6 h, during which time the color changed to red-purple. Solvent was removed *in vacuo*. The remaining pink solid was washed with diethyl ether (3 × 10 mL) and dissolved in dry MeOH (<10 mL), and fuchsia crystals of [Co(amine)Cl]Cl·1.75 MeOH suitable for X-ray analysis were formed from diethyl ether diffusion (yield 73%). Anal. Calcd (Found) for $C_{14}H_{29}N_3S_2CoCl_2$·1.75MeOH·H_2O: C, 37.4 (36.1); H, 7.50 (7.1). FTIR (KBr pellet): ν [cm^{-1}] = 3491, 3075, 1082. UV-vis in MeOH [λ_{max}, nm (ϵ)]: 308 (982), 486 (86), 736 (119).

(*S*,*S*′-(3-Aza-1,5-pentanediyl)-*N*,*N*′-bis(2-mercaptoethyl)-1,5-diazacyclooctane-*N*,*N*′,*N*″,*S*,*S*′)rhodium(III) Chloride, or [Rh(amine)-Cl]Cl$_2$. In a manner similar to that described for the cobalt complex, $RhCl_3$·*x*H_2O (0.056 g, 0.27 mmol) in anhydrous EtOH (20 mL) was added to 4,10-dithia-1,7,13-triazabicyclo[11.3.3]nonadecane (0.090 g, 0.30 mmol) dissolved in dry EtOH (20 mL). The reaction time of 30 min was sufficient to see a color change to bright yellow. Solvent was removed via vacuum. The solid yellow residue was washed with diethyl ether (3 × 10 mL) and dissolved in a minimal amount of dry MeOH (∼10 mL). Yellow-orange crystals of [Rh(amine)Cl]Cl_2 suitable for X-ray analysis were formed from diethyl ether diffusion (yield 66%). Anal. Calcd (Found) for $C_{14}H_{29}N_3S_2RhCl_3$·3H_2O: C, 29.66 (29.3); H, 6.22 (6.15). FTIR (KBr pellet): ν [cm^{-1}] = 3420, 1122. UV−vis in H_2O [λ_{max}, nm (ϵ)]: 388 (570).

^{105}Rh−N_3S_2 Complexation. The pH of the acidic rhodium(III)-105 chloride reagent was adjusted within the desired range of 2−9 by dropwise addition of NaOH, a 1 M solution initially, followed by a 0.05 M solution. To a 200 μL portion of the reagent solution containing *ca.* 0.5 mCi (18−19 MBq, *ca.* 3.4 × 10^{12} atoms of Rh) of ^{105}Rh were added 200 μL of ethanol and 100 μL of 50/50 acetonitrile/ethanol containing 10 μg of the N_3S_2 macrocycle. Control experiments were performed in which the rhodium(III)-105 chloride reagent was reacted as above with 100 μL of 50/50 acetonitrile/ethanol replacing the N_3S_2 ligand aliquot. The resultant solutions were heated at temperatures ranging from 50−80 °C for 1 h after mixing.

The effects of temperature and pH on ^{105}Rh-N_3S_2 complexation were determined. The pH was varied between 2 and 9. Buffers were not

(14) Lo, J. M.; Pillai, M. R. A.; John, C. S.; Troutner, D. E. *Int. J. Radiat. Appl. Instrum., Part A, Appl. Radiat. Isot.* **1990**, *41*, 103.

(15) Martell, A. E.; Motekaitis, R. J. *Determination and Use of Stability Constants*, 2nd ed.; VCH Publisher: New York, 1992.

(16) Mills, D. K.; Reibenspies, J. H.; Darensbourg, M. Y. *Inorg. Chem.* **1990**, *29*, 4364.

Table 1. Crystallographic Summary for [Ni(amine)Cl]Cl, [Co(amine)Cl]Cl, and [Rh(amine)Cl]Cl_2

	[Ni(amine)Cl]Cl	[Co(amine)Cl]Cl	[Rh(amine)Cl]Cl_2
chem formula	$C_{14}H_{29}N_3S_2NiCl_2$·MeOH	$C_{14}H_{29}N_3S_2CoCl_2$·1.75MeOH	$C_{14}H_{29}N_3S_2RhCl_3$
fw (g/mol)	465.17	489.68	512.78
space group	monoclinic, $P2_1/c$ (no. 14)	monoclinic, $P2_1/n$ (no. 14)	monoclinic, $C1c1$ (no. 9)
a (Å)	13.278(3)	10.321(2)	9.655(2)
b (Å)	11.976(4)	7.892(1)	16.805(4)
c (Å)	12.928(4)	27.684(3)	11.756(3)
β (deg)	102.17(2)	96.91(1)	96.29(2)
V (Å^3)	2009.6(10)	2238.6(6)	1896.0(8)
Z	4	4	4
ρ(calcd) (g cm^{-3})	1.538	1.453	1.796
temp (°C)	−110	−110	20
radiation (λ, Å)		Mo Kα (0.710 73)	
total no. of reflns	3728	4222	1791
no. of obsd reflns[a]	3555	3983	1754
	$I \geq 2.0\sigma I$	$I \geq 2.0\sigma I$	$I \geq 2.0\sigma I$
μ (cm^{-1})	0.1448	0.1206	0.1546
$R_w(F^2)$ (%)[a]	11.02	13.26	5.22
$S(F^2)$[a]	1.032	1.047	1.056

[a] Residuals: $R_{int} = [\sum F^2 - (F_{mean})^2]/[\sum F^2]$; $R = \sum|F_o - F_c|/\sum F_o$; $R_w(F^2) = \{\sum w(|F_o^2| - |F_c^2|)^2/\sum w(F_o^2)^2\}^{1/2}$; $S(F^2) = \{\sum w(F_o^2 - F_c^2)^2]/[N_{data} - N_{param}\}^{1/2}$.

used for pH control because several buffers were previously found to adversely affect complexation yields.[11] The effects of temperature on complex yields at pH 4 were measured by maintaining the reactions at 50, 70, and 85 °C. Some difficulty was encountered with ligand solubility (at the concentration used) at the lower temperatures.

The stability of the $^{105}Rh-N_3S_2$ complex in phosphate/citrate buffer (pH 7) was measured at 24 h intervals for 5 days. In these studies, 200 μL of the $^{105}Rh-N_3S_2$ reaction mixture containing *ca*. 0.2 mCi (7.4 MBq) of ^{105}Rh was added to 300 μL of 0.05 M phosphate buffer at pH 7 and room temperature. The $^{105}Rh-N_3S_2$ was not separated from the reaction mixture prior to assessment of stability. The percent complex remaining was determined by TLC and MgO adsorption.

Ion Exchanges. Anion exchanges used [Ni(amine)Cl]Cl (50 mg, 0.11 mmol) dissolved in MeOH (20 mL) and 10 equiv of NaSPh or 2 equiv of AgO_2CCH_3 in MeOH (10 mL). For each exchange, solutions of the Na^+ or Ag^+ salt were added via cannula and the solution was stirred under N_2 at room temperature overnight. The solutions were then filtered through Celite, and the solvent removed under vacuum. The powders were examined by mass spectroscopy and electrochemical analysis.

Reduction of [Ni(amine)Cl]Cl. The [Ni(amine)Cl]Cl complex (0.012 g, 0.03 mmol) was dissolved in 20 mL of dry ethanol, and 3.2 mL of a 0.1 M ethanolic solution of $NaBH_4$ was added via syringe. Within 60 s the solution turned green, and a sample for EPR was withdrawn and frozen in N_2(l). The solution stayed green at room temperature under N_2 for 2 h, after which a black precipitate formed.

Reduction and Oxidation of [Co(amine)Cl]Cl. A stock solution of [Co(amine)Cl]Cl was prepared by dissolving [Co(amine)Cl]Cl (20 mg, 0.04 mmol) in dry MeCN (10 mL). Reduction of [Co(amine)Cl]-Cl was accomplished by adding $NaBH_4$ (3 mg, 0.07 mmol) dissolved in EtOH (5 mL) to 5 mL of the stock solution via syringe. The color changed from pink to orange to yellow. A sample for EPR was immediately frozen in N_2(l). Another 5 mL portion of the stock solution of [Co(amine)Cl]Cl was used for oxidation by cerium(IV) ammonium nitrate, CAN, (13.4 mg, 0.02 mmol) dissolved in 5 mL of dry MeCN. In this case, the color changed from pink to blue as CAN was added, and an EPR sample was immediately prepared and frozen in N_2(l).

X-ray Crystallography and Structure Solution. The X-ray crystal structure analyses were carried out at the Crystal & Molecular Structure Laboratory Center for Chemical Characterization and Analysis at Texas A&M University. Crystallographic data for the complexes are listed in Table 1. Preliminary examinations and data collections were performed on a Rigaku AFC5 X-ray diffractometer. The structures were solved by direct methods [SHELXS, SHELXTL-93].[17]

(17) (a) Sheldrick, G. M. SHELXS-86, Institut fur Anorganische Chemie der Universitat, Göttingen, Germany, 1986. (b) Sheldrick, G. M. SHELXL-93, Institut fur Anorganische Chemie der Universitat, Göttingen, Germany, 1993.

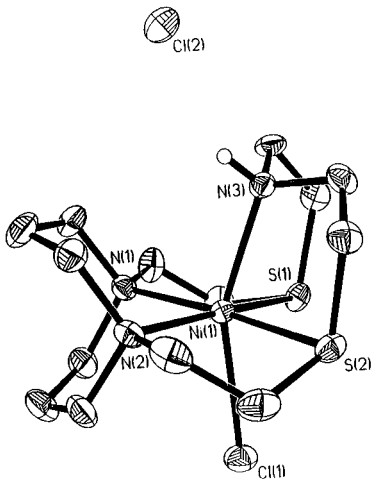

Figure 1. Thermal ellipsoid plot of [Ni(amine)Cl]Cl (thermal ellipsoids at 50% probability). MeOH of crystallization has been omitted for clarity.

Results and Discussion

The reaction of **Ni-1** with excess bis(2-chloroethyl)amine (eq 3) in CH_3CN yields a sky blue precipitate, [Ni(amine)Cl]Cl, which is soluble in protic solvents and CH_2Cl_2. It is insoluble in Et_2O, CH_3CN, and hydrocarbon solvents. Diethyl ether diffusion into a purple methanolic solution affords blue, hygroscopic crystals of [Ni(amine)Cl]Cl suitable for X-ray analysis. As isolated, six-coordinate [Ni(amine)Cl]Cl (Figure 1) contained one methanol molecule of crystallization. As observed with the N_2S_2OX derivatives of **Ni-1**, the Ni center in this N_3S_2 environment attracts a halide *trans* to nitrogen to complete its octahedral coordination sphere.[2,4]

The [Ni(amine)Cl]Cl complex was used as a precursor for the preparation of the Co^{II} and Rh^{III} derivatives. Removal of Ni^{II} from [Ni(amine)Cl]Cl in aqueous solution by addition of KCN and extraction with diethyl ether yields the free amine ligand 4,10-dithia-1,7,13-triazabicyclo[11.3.3]nonadecane (Scheme 2), which was used as isolated after vacuum removal of the Et_2O. Equivalent amounts of ligand and $CoCl_2$ or $RhCl_3$·xH_2O dissolved in MeOH or EtOH, respectively, were mixed with the ligand, producing a pink or yellow solution, respectively. Fuchsia crystals of [Co(amine)Cl]Cl and yellow crystals of [Rh(amine)Cl]Cl_2 suitable for X-ray analysis were obtained by diethyl ether diffusion into the alcoholic solutions. Experimental

Scheme 2

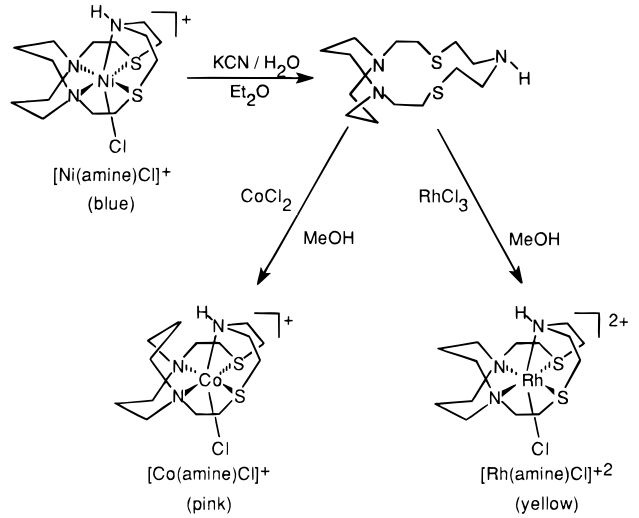

Table 2. Selected Bond Lengths (Å), Angles (deg), and Dihedral Angle[a] in the N_2S_2 Cavity (deg) for [Ni(amine)Cl]Cl, [Co(amine)Cl]Cl, and [Rh(amine)Cl]Cl_2

	[Ni-(amine)Cl]Cl	[Co-(amine)Cl]Cl	[Rh-(amine)Cl]Cl_2
M(1)−N(1)	2.138(4)	2.233(4)	2.112(4)
M(1)−N(2)	2.158(4)	2.199(4)	2.110(4)
M(1)−N(3)	2.175(4)	2.247(4)	2.085(4)
M(1)−S(1)	2.388(1)	2.529(1)	2.275(1)
M(1)−S(2)	2.391(2)	2.531(1)	2.268(1)
M(1)−Cl	2.547(1)	2.423(1)	2.406(2)
N(1)−M(1)−N(2)	83.5(2)	82.7(2)	85.8(2)
S(1)−M(1)−S(2)	99.8(5)	113.1(5)	93.9(5)
S(1)−M(1)−N(1)	88.1(1)	82.6(1)	89.9(1)
S(1)−M(1)−N(2)	169.5(2)	160.6(1)	175.2(1)
S(2)−M(1)−N(1)	171.5(1)	161.1(1)	175.4(1)
S(2)−M(1)−N(2)	88.5(1)	84.0(1)	90.3(1)
N(3)−M(1)−S(1)	82.9(1)	77.6(1)	88.1(1)
N(3)−M(1)−S(2)	82.1(1)	78.1(1)	87.6(1)
N(3)−M(1)−N(1)	103.8(1)	117.1(3)	95.2(2)
N(3)−M(1)−N(2)	100.0(1)	98.2(1)	94.5(2)
N(3)−M(1)−Cl	155.2(1)	144.5(1)	165.9(1)
Cl−M(1)−S(1)	82.1(5)	86.1(4)	82.6(6)
Cl−M(1)−S(2)	81.1(5)	79.8(5)	82.5(5)
Cl−M(1)−N(1)	95.4(1)	91.3(1)	95.4(1)
Cl−M(1)−N(2)	97.7(1)	106.7(1)	95.6(1)
dihedral angle[a]	4.9	15.5	3.4

[a] Defined as the angle between the NiN_2 and NiS_2 planes.

crystallographic data are found in Table 1 and a listing of selected bond lengths and bond angles are in Table 2 for complexes [Ni(amine)Cl]Cl, [Co(amine)Cl]Cl, and [Rh(amine)Cl]Cl_2; molecular structures are presented in Figures 1−3, respectively. Note that we have in Scheme 2 and in other places represented the S to axial N ethylene linkers as identical in all three complexes. In fact, the stick structures most resemble the Rh complex, Figure 3, while the Co and Ni complexes show a different conformer in one of the linkers.

The Ni^{II} and the Rh^{III} complex geometries are slightly distorted octahedrons. The least squares planes of N(1), N(2), S(1), and S(2) for [Ni(amine)Cl]Cl and for [Rh(amine)Cl]Cl_2 can be described as flat, with mean deviations from the plane for the named atoms of 0.032 and 0.002 Å, respectively.[18] The nickel atom is 0.060 Å from this N_2S_2 best plane while the rhodium is 0.046 Å. Comparitively, the least squares plane of

(18) The equation defining the least squares plane of N(1), N(2), S(1), and S(2) for [Ni(amine)Cl]Cl is $10.045x - 6.443y + 2.637z = 3.8658$, for [Rh(amine)Cl]$Cl_2$, $-4.237x + 2.486y + 10.922z = 0.4159$, and for [Co(amine)Cl]Cl, $4.714x + 6.660y - 9.257z = 6.712$.

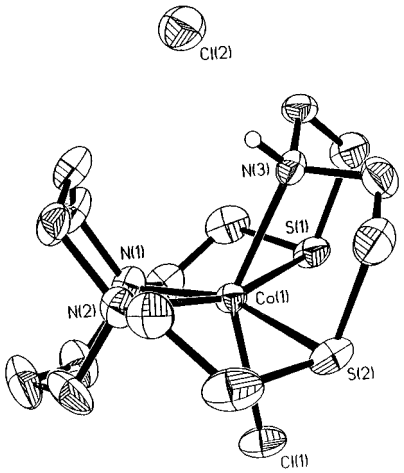

Figure 2. Thermal ellipsoid plot of [Co(amine)Cl]Cl (thermal ellipsoids at 50% probability). MeOH has been omitted for clarity.

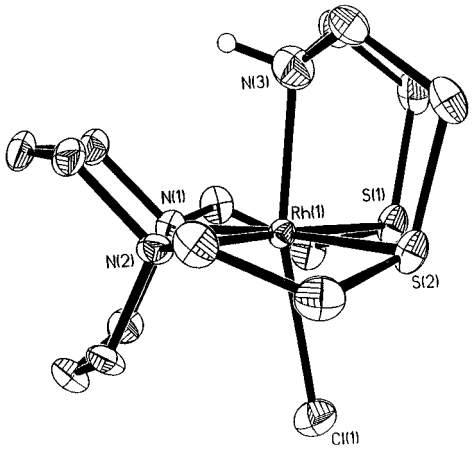

Figure 3. Thermal ellipsoid plot of [Rh(amine)Cl]Cl_2 (thermal ellipsoids at 50% probability). Cl^- counterions have been omitted.

N(1), N(2), S(1), and S(2) for [Co(amine)Cl]Cl is considerably warped, with a mean deviation from the plane for the named atoms of 0.225 Å, and for Co, 0.013 Å. In each of the metallic derivatives, the secondary amine folds over the N_2S_2 plane, placing N(3) in a metal-bound axial position, *trans* to the M−Cl bond. For [Ni(amine)Cl]Cl and [Rh(amine)Cl]Cl_2, the N(3)−M−Cl bond angles are 155.2(1)° and 165.9(1)°, respectively, while the analogous angle for M = Co is 144.5°.

Common to [Ni(amine)Cl]Cl and [Rh(amine)Cl]Cl_2 is the usual chair/chair conformation of the fused metalladiazacyclohexane rings observed, thus far, for all six-coordinate derivatives of **Ni-1**. In contrast, [Co(amine)Cl]Cl has a chair/boat conformation which is typical of four-coordinate complexes, but uncommon for a six-coordinate species of metallodiazacyclohexanes. Examination of the packing diagram reveals that solvent (MeOH) molecules occupy the area between the rows of complex molecules that stack along the *b* axis. Were these areas available, a normal chair/chair conformation would be sterically more favored. As it is, the CoN_2C_3 boat conformation places the β-methylene hydrogen to within 2.2 Å of the "axial" amine hydrogen, accounting for the small (144.5°) N(3)−Co−Cl bond angle. The N(2)−Co−Cl and N(2)−Co−N(3) bond angles [106.7(1)° and 117.1(3)°, respectively] are 15−20° larger than those of the N(1)−Co−Cl and N(1)−Co−N(3) angles [91.3(1)° and 98.2(1)°, respectively]. The overlay plots of the least squares fit of Ni, Co, S(1), and S(2) of the [Ni(amine)Cl]Cl and [Co(amine)Cl]Cl complexes (Figure 4) illustrate the essential structural differences between the two metal deriva-

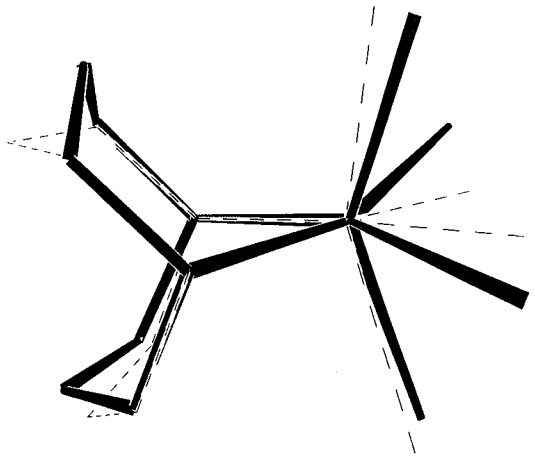

Figure 4. Overlay of the stick projections of $[Ni(amine)Cl]^+$ (- - -) and $[Co(amine)Cl]^+$ (—). N(1), N(2), Ni, and Co have been selected for least squares fit; all hydrocarbons except the daco backbone have been omitted for clarity.

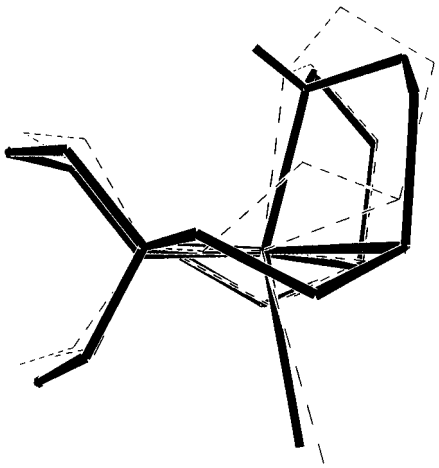

Figure 5. Overlay of the stick projections of $[Ni(amine)Cl]^+$ (—) and $[Ni(ether)I]^+$ (- - -); S(1), S(2), and Ni have been selected for least squares fit; all hydrogen atoms except the secondary amine hydrogen have been omitted for clarity.

tives. The S(1)−Co−S(2) bond angle has opened by *ca.* 13° as compared to the Ni derivative.

Overlay plots of the least squares fit of Ni, S(1), and S(2) of $[Ni(amine)Cl]^+$ and $[Ni(ether)I]^+$ (shown in eq 2), Figure 5, show that the most obvious distinction between these two complexes is that the ethylene arms linking the N and S donor atoms are eclipsed in the N complex and staggered in the O derivative.[3] It is also clear from the plots that the Ni, N(1), N(2) portion of the N_2S_2 coordination field in $[Ni(ether)I]^+$ shows larger deviation from planarity than the analogous $[Ni(amine)Cl]^+$ complex. In fact, the mean deviation in the NiN_2S_2 plane is 0.14 Å for the former and only 0.01 Å for the latter. The folded over portions of the ether and amine complexes are fairly similar. A significant difference lies in the Ni−O [2.387(5) Å] and Ni−N [2.175(4) Å] distances. This substantial difference also affects the Ni−S−CH_2CH_2-heteroatom rings; for $[Ni(amine)Cl]^+$ C(13)−C(14)−S(1) = 105.9(3)°, while for $[Ni(ether)I]^+$ C(13)−C(14)−S(1) = 113.4(5)°.

Spectroscopy. In aprotic solvents (*e.g.*, CH_2Cl_2), [Ni(amine)Cl]Cl forms blue solutions with absorptions at 384 ($\epsilon = 40$ M^{-1} cm^{-1}) and 596 nm ($\epsilon = 25$ M^{-1} cm^{-1}). When dissolved in protic solvents (H_2O, ROH), the color shifts to purple with absorptions at 366 ($\epsilon = 85$ M^{-1} cm^{-1}) and 568 nm ($\epsilon = 38$ M^{-1} cm^{-1}), consistent with a coordination change from six to four (eq 4).

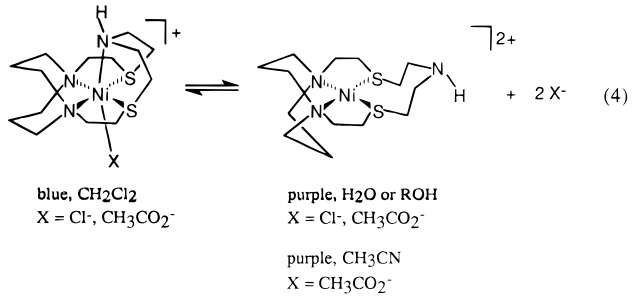

(4)

The complex [Co(amine)Cl]Cl is soluble in protic and polar aprotic solvents, forming pink to red solutions in all. It exhibits UV−vis absorptions at 486 nm ($\epsilon = 86$ M^{-1} cm^{-1}) and 736 nm ($\epsilon = 119$ M^{-1} cm^{-1}) and a charge transfer band at 308 nm ($\epsilon = 986$ M^{-1} cm^{-1}). Soluble in protic solvents and slightly soluble in MeCN and pyridine, $[Rh(amine)Cl]Cl_2$ remains yellow in solution and exhibits an absorption band at 388 nm ($\epsilon = 570$ M^{-1} cm^{-1}).

Ion Exchanges. In attempts to alter the coordination sphere about the Ni^{II} center of [Ni(amine)Cl]Cl, anion exchanges were carried out, making use of NaSPh and AgO_2CCH_3 (eq 5).

$$[Ni(amine)Cl]^+ \xrightarrow{MX} [Ni(amine)X]^+ + MCl \qquad (5)$$

$$MX = NaSPh,\ Ag[CH_3CO_2]$$

Methanolic solutions of [Ni(amine)Cl]Cl were stirred at room temperature under N_2 with NaSPh or AgO_2CCH_3 overnight. The $[Ni(amine)X]^+$ powders were examined by FAB^+ mass spectroscopy and electrochemical analysis.

The $[Ni(amine)Cl]^+$ species displays a parent signal at *m/z* 396, consistent with the formulation $C_{14}H_{29}N_3S_2NiCl$; a more intense signal at *m/z* 360 indicates the loss of chloride. Reaction of [Ni(amine)Cl]Cl with 10 equiv of NaSPh in MeOH produced an N_3S_3 donor set as evidenced by a color change from blue to green, solubility in CH_3CN, and a *m/z* signal at 471, corresponding to the mass of $[Ni(amine)SPh]^+$. Addition of 2 equiv of AgO_2CCH_3 to [Ni(amine)Cl]Cl results in the formation of a white precipitate, AgCl, which was removed by filtration. The Ni complex, which is blue in the solid state, exhibits a mass spectrum signal at *m/z* 420 consistent with the formulation $C_{16}H_{31}N_3OS_2Ni$. It displays C−O stretches in the infrared at 1593 and 1383 cm^{-1}, implying a $[Ni(amine)OAc]^+$ species is formed.

Electrochemistry and EPR. The cyclic voltammogram of [Ni(amine)Cl]Cl is shown in Figure 6. It exhibits an electrochemically quasi-reversible and chemically reversible reduction event ($E_c = -0.55$ V, $E_a = -0.45$ V vs NHE in EtOH) and no oxidation event when scanned to 0.80 V vs NHE, the limit of the solvent window (Table 3). In CH_2Cl_2, the reduction potential at −0.65 V is *ca.* 0.15 V more positive than the reduction in EtOH. An irreversible event, presumed to be $Ni^{II/III}$ oxidation, occurs at 2.13 V in CH_2Cl_2. The oxidation event occurs at a much more positive potential than known six-coordinate, thioether derivatives of **Ni-1**. For example, in CH_3CN solvent, the neutral, six-coordinate, **Ni-1** diacetate has a $Ni^{II/III}$ couple at 1.19 V[19] but no $Ni^{II/I}$ couple when scanned to −2.0 V. More similar to the redox behavior of $[Ni(amine)Cl]^+$ is the four-coordinate, dimethyl derivative of **Ni-1** which displays a $Ni^{II/I}$ reduction and a $Ni^{II/III}$ oxidation at −0.48 V

(19) Goodman, D. C.; Tuntulani, T.; Farmer, P. J.; Darensbourg, M. Y.; Reibenspies, J. H. *Angew. Chem., Int. Ed. Engl.* **1993**, *32*, 116.

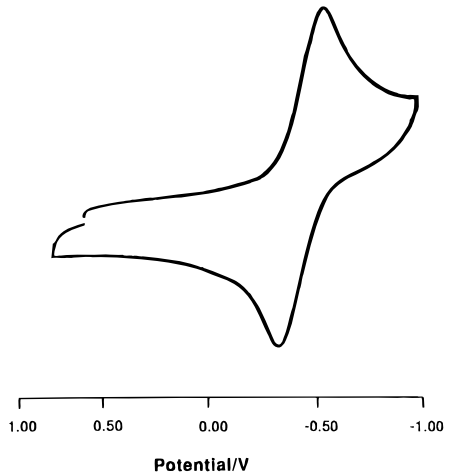

Figure 6. Cyclic voltammogram of [Ni(amine)Cl]Cl (2 mM) in EtOH scanned toward negative potential at a rate of 200 mV/s: saturated ethanolic solution of LiBr; $E_{1/2} = -0.50$ V (vs NHE), with $\Delta E_{a/c} = 0.10$ V, $i_{pa}/i_{pc} = 1.00$.

Table 3. Redox Potentials and Reversibility Data from Cyclic Voltammetry[a]

			complex reduction			complex oxidation		
compound	solvent	color	$E_{1/2}$ (V)	ΔE (V)	i_{pa}/i_{pc}	E_a (V)	ΔE (V)	i_{pa}/i_{pc}
[Ni(amine)Cl]Cl	EtOH[a]	purple	−0.50	0.10	1.00			
[Ni(amine)Cl]Cl	CH_2Cl_2[b]	blue	−0.65	0.20	0.01	2.13[c]		
[Ni(amine)SPh]$^+$	EtOH[a]	green	−0.55	0.10	0.80	0.79[d]		
[Ni(amine)SPh]$^+$	CH_3CN[b]	green	−0.98	0.11	0.89	0.45[d]		
[Ni(amine)OAc]$^+$	EtOH[a]	purple	−0.50	0.08	0.80			
[Co(amine)Cl]Cl	DMF[b]	pink	−1.24	0.08	1.55	0.27	0.09	1.40

[a] Data obtained in 0.1 M LiBr with a glassy carbon working electrode at 200 mV/s; scale referenced to NHE. [b] Data obtained in 0.1 M $[Bu_4N][PF_6]$ with a glassy carbon working electrode at 200 mV/s; scale referenced to NHE. [c] Irreversible oxidation, assumed to be $Ni^{II/III}$. [d] Irreversible oxidation, assumed to be $RS^- \rightarrow RS^{\bullet}$.

and 1.57 V, respectively.[20] The dicationic charge of dimethyl-**Ni-1** plays a major role in the ease of $Ni^{II/I}$ accessibility, and a

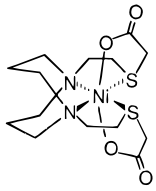

diacetate-**Ni-1**

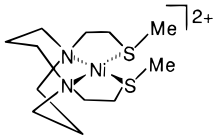

dimethyl-**Ni-1**

strict comparison to the monocationic [Ni(amine)Cl]$^+$ must include conductivity measurements. In fact conductivity measurements of dimethyl-**Ni-1** as its iodide salt in CH_3CN solvent imply extensive ion-pairing, and a solution structure of [dimethyl-**Ni-1**(I)]$^+$ is probably appropriate. Therefore, the cyclic voltammetry data of [Ni(amine)Cl]Cl are most consistent with the loss of axial amine coordination, giving rise to a N_2S_2-(thioether)Cl$^+$ environment similar to the [dimethyl-**Ni-1**(I)]$^+$ complex.

In contrast to the mobility of the folded over amine donor of [Ni(amine)Cl]Cl, a similar pentadentate P_2S_2N derivative, [bis-(5-(diphenylphosphino)-3-dithiapentyl)amine]nickel(II) tetrafluoroborate, shows no loss of the axial nitrogen donor in solution. The stability of Ni^I ($Ni^{II/I}$ redox couple at −0.21 V vs SCE) within this soft ligand field permits isolation and crystal structure analysis of the Ni^I complex.[21]

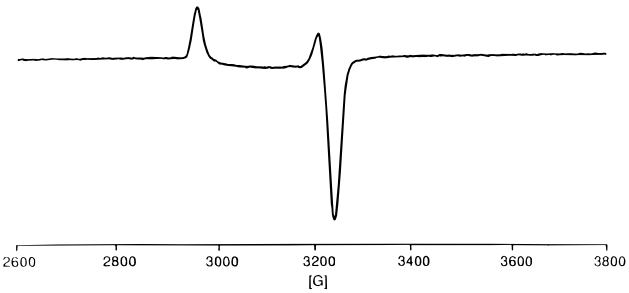

Figure 7. X-band EPR spectra for [Ni(amine)Cl]Cl: data collected at 10 K ($\nu = 9.432$ GHz) in anhydrous EtOH (1.29 mM) after reduction with $NaBH_4$. Calculated g values: 2.09, 2.27.

Bulk chemical reduction of [Ni(amine)Cl]Cl at room temperature in EtOH with $NaBH_4$ resulted in a green solution. A frozen sample (−78 °C) of this solution exhibits an axial EPR signal (Figure 7) with calculated g values: 2.09, 2.27. Such data are typical of an unpaired electron in the $d_{x^2-y^2}$ orbital of a square planar Ni^I species.[3,22a,b]

Both the geometry around the nickel center and the counterion affect the redox potential of [Ni(amine)Cl]Cl (Table 3). In protic solvents, the salts of [Ni(amine)Cl]Cl, assumed to contain four-coordinate nickel, show reversible to quasi-reversible $Ni^{II/I}$ reductions. As expressed in eq 5, the salts are all purple in these solutions, with the exception of the green $^-$SPh salt, and the reduction potentials occur between −0.50 and −0.55 V. In polar aprotic solvents, the derivatives are blue (six-coordinate), with the exception of the green $^-$SPh salt, and the reduction events are shifted to more negative potentials between −0.65 and −0.98 V. In addition, an irreversible oxidation event is observed for the six-coordinate analogs of [Ni(amine)Cl]Cl, but not for the four-coordinate species.

Reasonable structures for the [Ni(amine)SPh]$^+$ complex which maintain SPh^- coordination as indicated by mass spectroscopy are shown below.

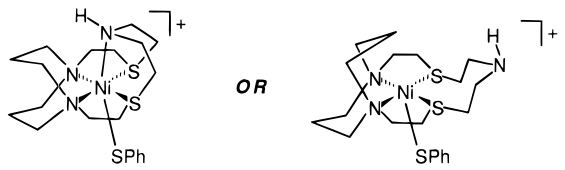

green in H_2O, ROH, and CH_2Cl_2

Since the known and transient five-coordinate complexes of Ni^{II} containing an N_2S_2 donor set are green, the most likely structure is five-coordinate with the thiolate bound and the amine unbound.[5,23]

In DMF, [Co(amine)Cl]Cl displays a $Co^{II/I}$ quasi-reversible redox couple at −1.24 V and a quasi-reversible $Co^{II/III}$ couple at 0.27 V (Figure 8, Table 3). The EPR spectrum of [Co(amine)Cl]Cl in MeCN is isotropic (Figure 9). Bulk chemical oxidation with cerium(IV) ammonium nitrate in MeCN produces a color change from pink to yellow. The frozen yellow species was EPR silent as expected for Co^{III}. However, attempts to obtain [Co(amine)Cl]Cl_2 in crystalline form have to date been unsuccessful.

(20) Farmer, P. J.; Reibenspies, J. H.; Lindahl, P. A.; Darensbourg, M. Y. *J. Am. Chem. Soc.* **1993**, *115*, 4665.

(21) James, T. L; Lisheng, C.; Muetterties, M. C.; Holm, R. H. *Inorg. Chem.* **1996**, *35*, 4148.

(22) (a) Lovecchio, F. V.; Gore, E. S.; Busch, D. H. *J. Am. Chem. Soc.* **1974**, *96*, 3109; (b) Suh, M. P. *Adv. Inorg. Chem.* **1997**, *44*, 93.

(23) Buonomo, R. M.; Reibenspies, J. H.; Darensbourg, M. Y. *Chem. Ber*. **1996**, *129*, 779.

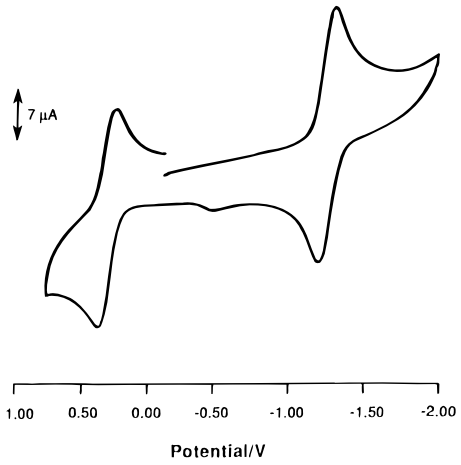

Figure 8. Cyclic voltammogram of [Co(amine)Cl]Cl (2 mM) in MeCN scanned toward negative potential at a rate of 200 mV/s (0.1 M [*n*-Bu_4N][PF_6]; $Co^{II/I}$, $E_{1/2} = -1.24$ V (vs NHE), with $\Delta E_{a/c} = 0.08$ V, $i_{pa}/i_{pc} = 1.55$; $Co^{II/III}$, $E_{1/2} = 0.27$ V (vs NHE), with $\Delta E_{a/c} = 0.09$ V, $i_{pa}/i_{pc} = 1.40$).

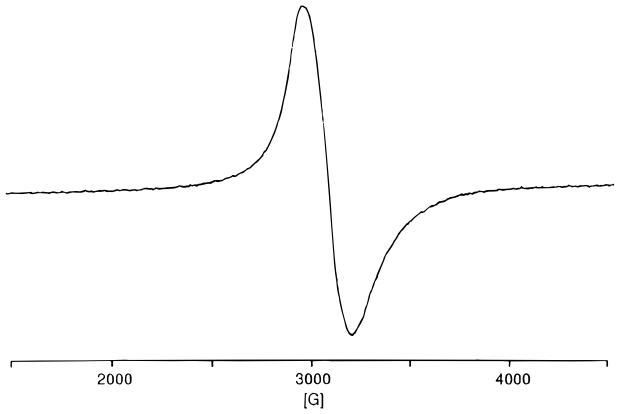

Figure 9. X-band EPR spectra for [Co(amine)Cl]Cl: data collected at 10 K ($\nu = 9.433$ GHz) in anhydrous MeCN (4.08 mM). Calculated *g* value: 2.20.

Radiochemistry. At the radiotracer level, rhodium(III)-105 chloride was found to complex the N_3S_2 ligand in greater than 98% yield (as determined by TLC and MgO adsorption) in 1 h at pH 5 and 80 °C. Ethanol was found to be essential to achieve high yields.[11] It has been proposed that ethanol catalyzes the complexation of Rh(III) by reducing small quantities of Rh(III) to Rh(I), which is kinetically more labile,[24] followed by reoxidation to the kinetically inert Rh(III) by atmospheric oxygen. This scenario is, however, unlikely in the bulk chemical studies described above.

The electrophoretic behavior of $[^{105}Rh(amine)Cl]^{2+}$ indicated that a cationic complex migrated as a single species toward the cathode. In the control experiments, the rhodium(III)-105 chloride reagent was treated analogously as in complex formation; it behaved as a neutral species remaining at the origin. Although the acidic rhodium(III)-105 chloride reagent is a mixture of anionic chloro−aqua species, this is no longer the case after reaction under complexation conditions.[11] Two chromatographic methods were developed using silica TLC that allowed differentiation of $[^{105}Rh(amine)Cl]^{2+}$ and the unreacted rhodium(III)-105 chloride reagent; the use of 50/50 chloroform/methanol as the eluent gave the optimal separation with the complex migrating near the solvent front (R_f 0.9−1) and the uncomplexed ^{105}Rh remaining at the origin. When saline was used as the eluent, the complex did not migrate as a "clean" spot but streaked with the majority of the radioactivity observed between R_f 0.3 and R_f 0.6. The complexation yield of $[^{105}Rh(amine)Cl]^{2+}$ was consistent by all three methods of analysis (TLC, electrophoresis, and MgO adsorption).

Table 4. Effect of Temperature and pH on the Yield of $[^{105}Rh(amine)Cl]^{2+}$ the Complex at a 1 h Reaction Time

temp (°C)	pH	% complexn	temp (°C)	pH	% complexn
50	4	33	80	4[a]	>90
70	4	72	80	5[a]	>98
85	4	>90	80	8[a]	10
80	2[a]	15			

[a] This is the pH of the rhodium(III)-105 chloride solution prior to addition of ethanol and the ligand solution.

The results of the temperature studies (Table 4) show that complexation in aqueous solution occurs best at 80 °C or greater; however, reaction times longer than the 1 h protocol might have produced higher complexation yields at lower temperatures. The pH/solvent composition must be optimized (to eliminate ligand precipitation at lower temperatures), and may afford a preparation that yields >90% complexation at temperatures below 65 °C, thereby making the reaction conditions more biocompatible. The results of the pH studies (Table 4) indicate that between pH 4 and pH 7 the complexation yields were >90%, which would provide flexibility in preparing complexes once the N_3S_2 is preconjugated to a biomolecule. Potentiometric titrations of the free ligand indicated that the monoprotonated ligand has a pK_a value of 7.2. A search of the *NIST Critically Selected Stability Constants of Metal Complexes* found no entries for another N_3S_2 ligand in aqueous media;[25a] however, the value of 7.2 lies within the reported range for macrocyclic ligands containing two secondary N and two S heteroatoms.[25bc26]

The stability of $[^{105}Rh(amine)Cl]^{2+}$ was investigated in pH 7 phosphate/citrate buffer incubated at room temperature. As determined by the TLC and MgO adsorption methods described above, over 95% of the complex remained after 5 days. Such excellent stability is consistent with the high thermodynamic and kinetic stability observed for Rh(III) complexes with a variety of ligands.[25]

Conclusions

Both the N and O pentadentate, macrocyclic derivatives of **Ni-1** lead to six-coordinate complexes in the solid state, $[Ni(ether)I]^+$ and $[Ni(amine)Cl]^+$ (eqs 2 and 3). Despite the indication from crystallographic metric data of a stronger "folded over" influence of N as an axial donor in comparison to O, the experimental probes used in our solution studies indicate the complexes undergo the 6−4 equilibrium equally well. An exact comparison cannot be made because of the difference in *trans*-halides.

The [Co(amine)Cl]Cl and [Ni(amine)Cl]Cl complexes demonstrate surprising structural differences within the macrocyclic ligand; the former shows greater deviation from octahedral geometry than the latter as well as an uncommon conformation in the coordinated daco rings. Both complexes show redox

(24) (a) Rund, J. V.; Basolo, F.; Pearson, R. G. *Inorg. Chem.* **1964**, 3, 658. (b) Gillard, R. D.; Osborn, J. A.; Wilkinson, G. *J. Chem. Soc.* **1965**, 1951. (c) Basolo, F.; Pearson, R. G. *Mechanisms of Inorganic Reactions*; Wiley: New York, 1967; pp 496, 605. (d) Addison, A. W.; Guillard, R. D.; Vaughan, H. *J. Chem. Soc., Dalton Trans.* **1973**, 1187.

(25) (a) NIST Standard Reference Database 46 (*NIST Critically Selected Stability Constants of Metal Complexes: Version 2.0*, NIST, Gaithersburg, MD, 1995). (b) Micheloni, M.; Paoletti, P.; Siegfried-Hertli, L.; Kaden, T. A. *J. Chem. Soc., Dalton Trans.* **1985**, 1169. (c) Arnaud-Neu, F.; Almasio, M. C.; Spiess, B.; Schwing-Weill, Sullivan, S. A.; Lehn, J. M. *Helv. Chim Acta* **1985**, *68*, 831.

(26) Jardine, F. H.; Sheridan, P. S. In *Comprehensive Coordination Chemistry*; Wilkinson, G., Gillaro, R. D., McLeverty, J. A., Eds.; Pergamon Press: Tarrytown, NY, 1987; Vol. 4, pp 901−1096.

Chart 1

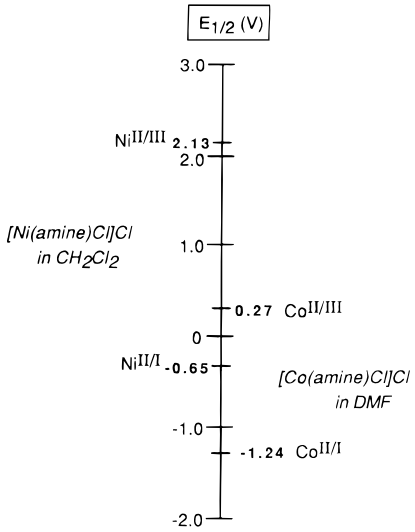

activity, giving rise to odd oxidation states, M^{I} and M^{III}. However, as summarized in Chart 1, $Co^{I/III}$ spans a smaller potential range (1.5 V) than $Ni^{I/III}$ (2.8 V).

The N_3S_2 macrocyclic ligand shows promise as a chelating agent for Rh^{III}. Radiotracer studies indicate that a solution of the ligand exposed to low concentrations of ^{105} Rh^{III} forms a cationic complex, which is consistent with the observation of $[^{103}Rh(amine)Cl]Cl_2$ at the macroscopic level. However, it remains to be determined whether all three nitrogen atoms (as is the case for the macroscopic complex) or just two nitrogen atoms are coordinated to the Rh^{III} at the tracer level. Both modes of ligand complexation would yield a cationic complex. The further derivatization of the ligand at the N−H functionality, as expressed in Scheme 1, remains a synthetic target.

Acknowledgment. Financial support from the National Science Foundation (Grant CHE 94-15901) is gratefully acknowledged. Funding for the X-ray diffractometer and crystallographic computing system (Grant CHE 8513273) was provided by the National Science Foundation. We thank Sheila Eng and Dr. Arthur Martell for use of the titration equipment and computer time, and Jason Smee for his help.

Supporting Information Available: A summary of structure determination and solution refinement; tables summarizing crystallographic data for [Ni(amine)Cl]Cl, [Co(amine)Cl]Cl, and $[Rh(amine)Cl]Cl_2$, atomic coordinates and isotropic displacement parameters, bond lengths, bond angles, anisotropic displacement parameters, H-atom coordinates and isotropic displacement parameters, and torsion angles less those to hydrogen atoms; crystal structure with thermal ellipsoids; and packing diagrams for [Ni(amine)Cl]Cl, [Co(amine)Cl]Cl, and $[Rh(amine)Cl]Cl_2$ (21 pages). See any current masthead for ordering and Internet access Instructions.

JA964187Z